

3D Simulation of Flows Around Hydraulic Structures

Tran Ngoc Anh, Shinichiro Onda, Nguyen Duc Hanh* and Nguyen Thanh Son

*e-mail address of presenting authors: hanhnd.vnu@gmail.com

Abstract: *Hydraulic structures have become popular tools for river training and bank protection. In many cases, groins or spur-dykes have had impressive effects on controlling sediment deposition for bank protection, or increasing water depth for navigation channels. Spur-dyke designs have generally been based on 2D calculations of flow structure and sediment transport. In some rivers where flood surge could make a significant difference in water level resulting in an over-topping phenomenon, these 3D aspects of flow structure may also cause additional harmful effects such as local scouring at the abutment, or river bank collapse. In these cases the 3D simulation of flow structure is needed to provide fundamental information for sediment transport and in order to examine solutions for these problems.*

This study deals with an application of a 3D hydraulic model based on RANS equations with turbulent closure using a non-linear $k-\epsilon$ model, to simulate the flow structure around hydraulic structures. Basic flow equations with contravariant velocity in a generalized curvilinear coordinate system are solved and a moving coordinate technique for vertical direction is used to calculate water surface variation. The simulation results were then compared with previous experimental results in the laboratory to show that this model is reasonably capable of reproducing results obtained in the field.

Key Words: 3D flow simulation, hydraulic modeling, submerged spur-dykes/groins

1. Introduction

In meandering rivers, hydraulic structures such as spur dykes (or groins) are common tools used to protect erodible banks, however, not all spur-dykes have worked as intended, particularly

in rivers experiencing significant differences in water level; in such cases overtopping can occur and cause harmful effects. In these cases, the complicated three-dimensional nature of flow around hydraulic structures must be taken into account.

For active management of rivers, reliable prediction tools (models) are essential for comparison of the expected performance of alternative hydraulic structure designs. When something more usually using an analytical solution is too difficult, physical and numerical models have been used to address sediment transport problems (Chanson, 1999).

Over the past few decades, problems related to flow and bed deformation processes around river hydraulic structures have been studied, mostly by physical modeling of spur-dykes, abutments, or bridge piers. Spur-dykes and abutments have been found to be alike due to their relatively similar shapes. The investigations on this type of obstruction have been presented by Melville (1992); Kwan and Melville (1994); Lim (1997); Rahman et al. (1998); and Kuhnle et al. (1999). The physical modeling experiments have also allowed close examination of flow characteristics and have been examined (Garde et al. 1961; Melville 1992), but the exact mechanism of how a submerged spur-dyke impacts the surrounding flow behavior is still not fully understood.

Numerical models are useful tools that can solve the basic equations of fluid hydrodynamics (Martin and McCutcheon, 1999) and can be used for prediction and further examination of flow behavior. Fluid mechanics equations can be solved in one-dimensional, two-dimensional or three-dimensional (3D) spatial schemes (Martin and McCutcheon, 1999). Solving these equations in their three-dimensional form is extremely difficult and has become feasible only as increased computer power makes numerical

solutions practical (Martin and McCutcheon, 1999). Recently, several numerical models have been developed to calculate the phenomena around river hydraulic structures. However, the number of test cases used to validate these numerical models is not adequate in understanding their general applicability to river hydraulic structures (Nagata et al., 2005).

This study deals with an application of a 3D hydraulic model based on Reynolds-averaged Navier-Stokes equations with a non-linear k- ε model for turbulent closure, to simulate the flow structure around hydraulic structures. The basic flow equations with contravariant velocity in a generalized curvilinear coordinate system were solved and a moving coordinate technique in the vertical direction was used to calculate water surface variation. The simulation results were then validated against the laboratory experiment results of Tominaga et al. (2000).

2. Numerical Method

A 3D simulation was conducted using the Reynolds averaged 3D flow equations with contravariant components of velocity vectors in a moving generalized curvilinear coordinate system (Kimura et al., 2004). These are described in Eqs (1)-(4).

[Continuity equation]

$$\frac{1}{\sqrt{g}} \frac{\partial V^\alpha \sqrt{g}}{\partial \xi^\alpha} = 0 \quad (1)$$

[Momentum equation]

$$\begin{aligned} \frac{\partial V^i}{\partial t} + \nabla_j [V^i (V^j - W^j)] + V^i \nabla_j W^j + V^j \nabla_j W^i \\ = F^i - \frac{1}{\rho} g^{ij} \nabla_j p + \nabla_j \left[-\overline{v^i v^j} \right] + 2\nu \nabla_j e^{ij} \end{aligned} \quad (2)$$

[k equation]

$$\begin{aligned} \frac{\partial k}{\partial t} + \nabla_j [k (V^j - W^j)] + k \nabla_j W^j \\ = -g_{il} \overline{v^l v^j} \nabla_j V^i - \varepsilon + \nabla_j \left\{ \left(\frac{D_t}{\sigma_k} + \nu \right) g^{ij} \nabla_i k \right\} \end{aligned} \quad (3)$$

$$\nabla_j [V^j k] = \frac{\partial V^j k}{\partial \xi^j} + V^m k \Gamma_{mj}^j \quad (4)$$

[ε equation]

$$\begin{aligned} \frac{\partial \varepsilon}{\partial t} + \nabla_j \left[\varepsilon (V^j - W^j) \right] + \varepsilon \nabla_j W^j = -C_{\varepsilon 1} \frac{\varepsilon}{k} g_{il} \overline{v^l v^j} \nabla_j V^i \\ - C_{\varepsilon 2} \frac{\varepsilon^2}{k} + \nabla_j \left\{ \left(\frac{D_t}{\sigma_k} + \nu \right) g^{ij} \nabla_i \varepsilon \right\} \end{aligned} \quad (5)$$

where ξ^j = generalized curvilinear coordinate; V^i = contravariant component of the velocity vector of flow; t = time; W^i = contravariant component of the velocity vector of grid motion; p = pressure; ν = molecular dynamic viscosity; ρ = density of water; k = turbulent energy; ε = turbulent energy dissipation rate; g_{ij} and g^{ij} = covariant and contravariant component of metric tensor; $g = \det(g_{ij})$; F^i = contravariant component of gravitational acceleration; and ∇^i indicates a co-variant differential.

A 2nd order non-linear k- ε model was adopted as a model which is appropriate for non-homogenous and anisotropic turbulent flows. This model has been applied to various flow fields, such as the swirling flows around submerged spur dikes (Kimura et al. 2004). The constitutive equations are described in Eqs (6)-(12) as follows:

$$-\overline{v^i v^j} = D_t S^{ij} - \frac{2}{3} k g^{ij} - \frac{k}{\varepsilon} D_t [\alpha_1 Q_1 + \alpha_2 Q_2 + \alpha_3 Q_3] \quad (6)$$

$$D_t = C_\mu \frac{k^2}{\varepsilon} \quad (7)$$

$$Q_1 = S^{i\alpha} g_{\alpha l} \Omega^{lj} + S^{j\beta} g_{\beta l} \Omega^{li} \quad (8a)$$

$$Q_2 = S^{i\alpha} g_{\alpha l} S^{lj} - \frac{1}{3} S^{k\alpha} g_{\alpha m} S^{m\beta} g_{\beta k} \delta_l^i g^{lj} \quad (8b)$$

$$Q_3 = \Omega^{i\alpha} g_{\alpha l} \Omega^{lj} - \frac{1}{3} \Omega^{k\alpha} g_{\alpha m} \Omega^{m\beta} g_{\beta k} \delta_l^i g^{lj} \quad (8c)$$

$$S^{ij} = g^{j\alpha} \nabla_\alpha V^i + g^{i\alpha} \nabla_\alpha V^j \quad (9a)$$

$$\Omega^{ij} = g^{j\alpha} \nabla_\alpha V^i - g^{i\alpha} \nabla_\alpha V^j \quad (9b)$$

$$\alpha_1 = -0.1325 f_M, \alpha_2 = 0.0675 f_M, \alpha_3 = -0.0675 f_M \quad (10a)$$

$$f_M = \frac{1}{1 + 0.02 M^2}, M = \max[S, \Omega] \quad (10b)$$

$$S = \frac{k}{\varepsilon} \sqrt{\frac{1}{2} S^{i\alpha} g_{\alpha j} S^{j\beta} g_{\beta i}}, \Omega = \frac{k}{\varepsilon} \sqrt{\frac{1}{2} \Omega^{i\alpha} g_{\alpha j} \Omega^{j\beta} g_{\beta i}} \quad (11)$$

$$C_{\mu} = \min \left[0.09, \frac{0.3}{1 + 0.09M^2} \right] \quad (12)$$

Eq. (10) was adjusted by considering the distribution of turbulent intensities in a simple shear flow in comparison with the previous experimental results (Kimura & Hosoda, 2000). Eq. (12) was determined to satisfy the reliability in a simple shear flow and the singular points in both 2D and 3D flow fields.

The governing equations were solved by applying the finite volume method on a full-staggered grid system. The QUICK scheme was used for the convection terms (Leonard, 1979) and the central differencing is applied for the diffusion terms of the momentum equations. The hybrid central upwind scheme was applied to the k and ϵ equations. The pressure field was solved using the iterative solution algorithm (SOLA) of Hirt et al. (1975), and the wall function approach was applied for the wall boundary conditions for k and ϵ . The free surface elevation was calculated using Eq. (13) (Takizawa et al. 1992).

$$\Delta h = \sqrt{g_{33}} V^3 \Delta t \quad (13)$$

where Δt = time increment and Δh = the change in surface elevation during Δt .

3. Application and Discussion

The model was verified using the laboratory experiment carried out by Tominaga et al. (2000). In this experiment (Figure 1), two spur dikes were installed in the left side of an open rectangular channel, which was 8m long, 0.3m wide (B) and its bed slope (i) was 1/2000.

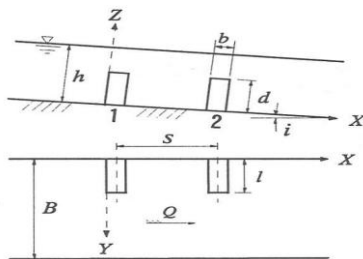


Figure 1. The set up of the experimental model.

The transverse length (l) of each spur dike was 0.05m; longitudinal thickness of each spur dike (b) was 0.02m; and the distance between them (S) was 0.1m. The spur dikes' height (d) were 0.02, 0.03, 0.04, 0.05, 0.06m (submerged cases) and

0.08m (emerged case) corresponding to SD2, SD3, SD4, SD5, SD6 and SD8.

The upstream inflow discharge (Q) and downstream water depth were kept constant as 4.1 l/s and 0.08m. All the above experiment conditions were simulated using the developed model, within a grid consisting of 321 x 61 x 17 cells in the longitudinal, transverse and vertical directions of the channel (Figure 2) with a higher resolution of cells nearest the modelled spur-dykes.

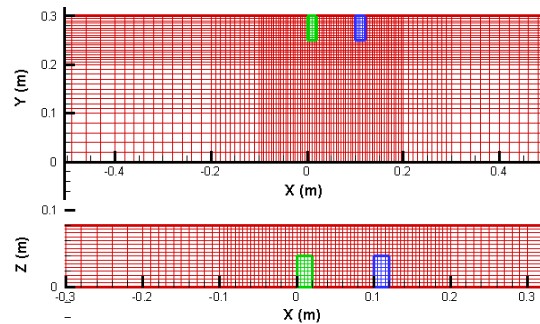


Figure 2. Computational grid: Upper: plan view (x-y) Lower: side view (x-z)

Figure 3 shows time-averaged images of the velocity vector of flow in a steady state. The vertical large-scale vortex generation between the spur dikes was well reproduced by the simulations, including the impacts of the increased spur dikes' height, including increased size of the vortex, increased velocity and movement of the vortex-core downstream. Simulations also replicated the flow behavior upstream of the first dike, where flow was split into two parts: one tending upward from the dike crest and the other going downward, potentially causing a horseshoe vortex and local scouring. These upstream vortices were intensified with the increase of the dike's height but almost disappeared in the emerged case (SD8).

Horizontal vortices were also reproduced well, as can be seen in the plan view of the velocity field at the half-depth of the spur dikes, shown in Figure 4. The horizontal eddies occur in all cases of simulation and were stronger in SD6 and SD8, potentially lead to more severe local scouring at spur dykes' toe.

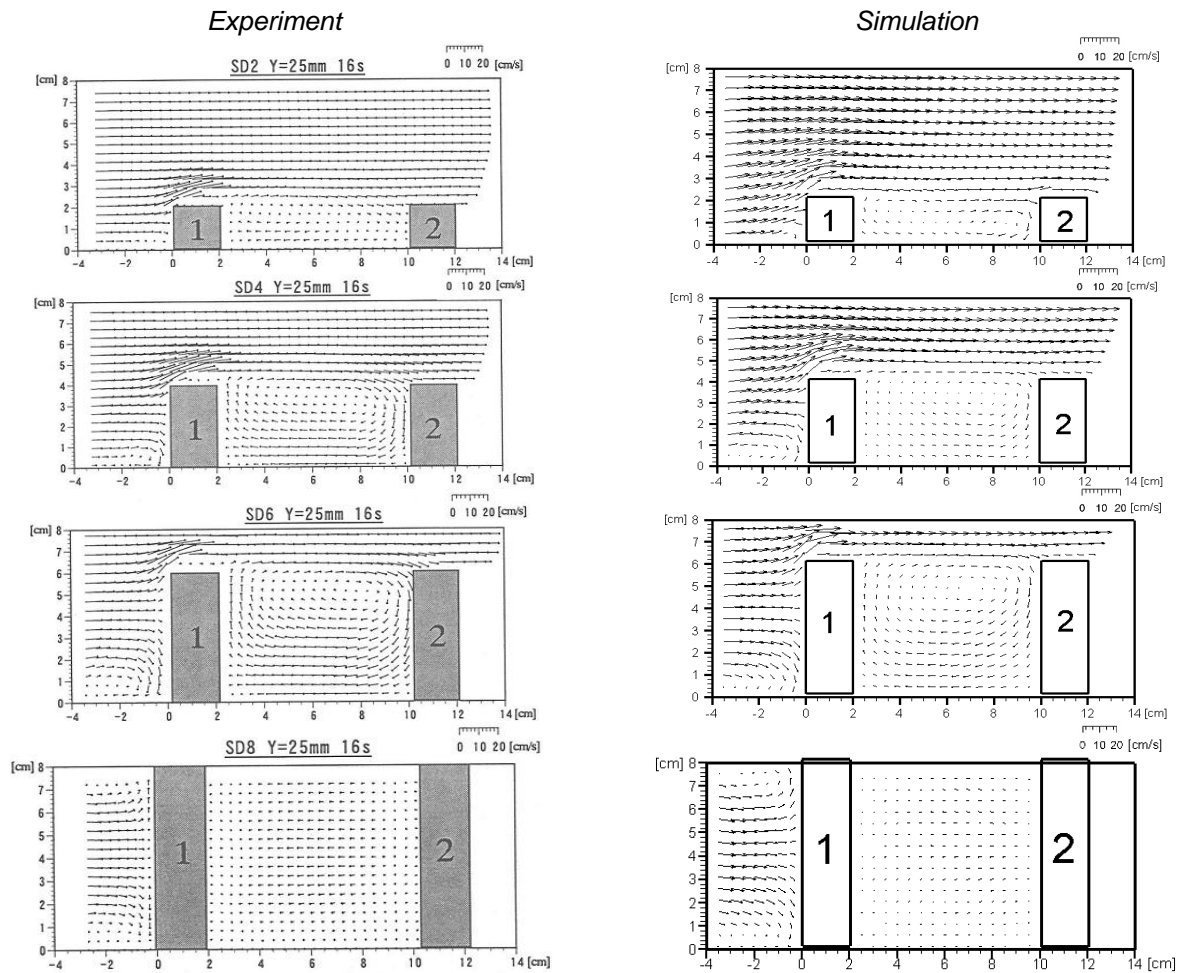


Figure 3. Velocity vector fields on Y-section. *Left*: measurement results; *Right*: simulation results

The velocity field in Figure 5 demonstrates that the adverse flow was generated near the channel bank with quite a strong over-topping flow and vortices between spur dikes (Figure 5 - upper), which might be a reason for channel bank scouring near dike abutments, but this was not observed in the region near the tip of the dikes (Figure 5 - lower). At the same time, a downward flow was displayed in the front of the second spur dike's tip (Figure 5), which might also cause a local scour hole at the dyke's toe. These characteristics were confirmed by the occurrence

of a large eddy near the bed layer as shown in Figure 6. Moreover, the harmonies of velocity distribution between measurement and simulation results are also revealed as shown in Figure 7.

All the above characteristics of flow structure were simulated in fair agreement with the measurement results from Tominaga et al. (2000), hence validating the capacity of the numerical model in simulation of the 3D nature of flow fields around submerged spur dikes.

Experiment

Simulation

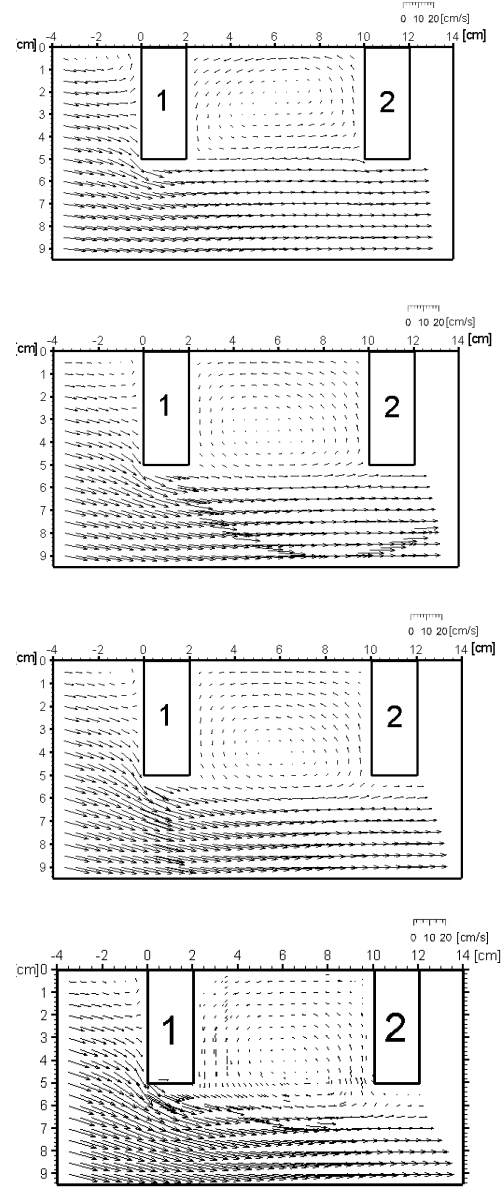
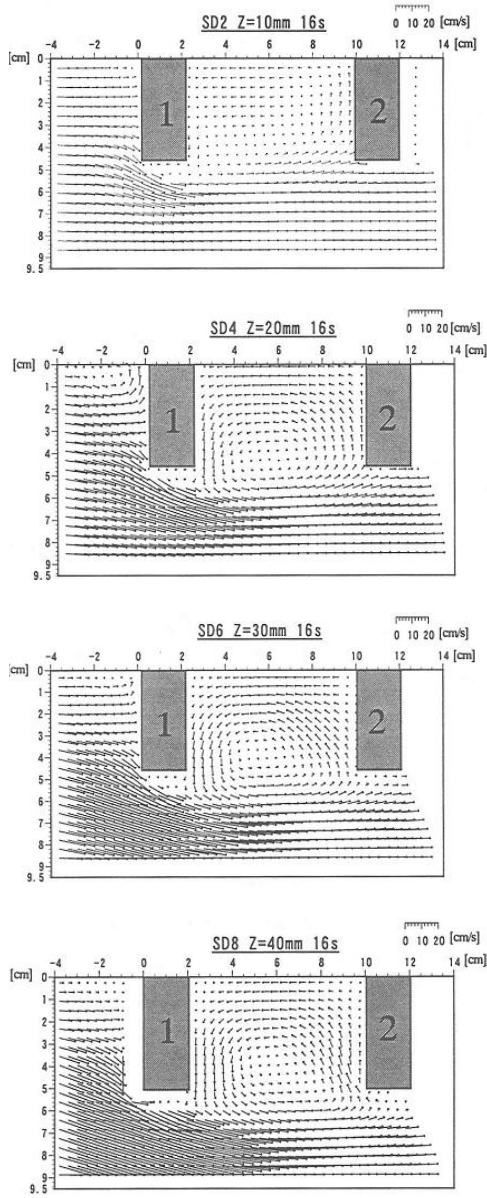


Figure 4. Velocity vector fields on Z-section. *Left*: measurement results; *Right*: simulation results

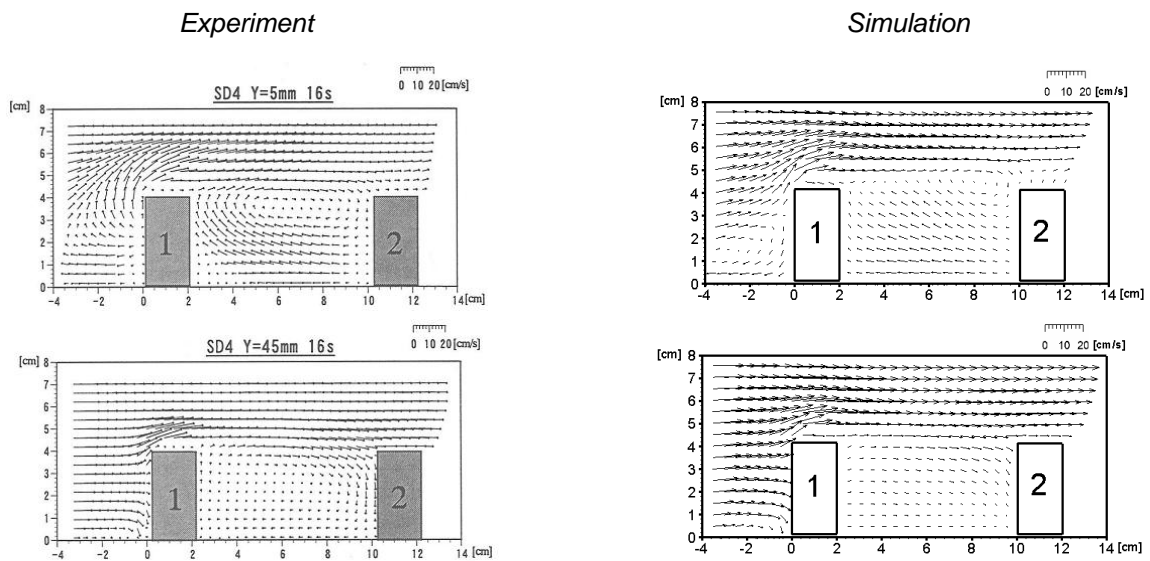


Figure 5. Velocity vector fields on Y-section. Left: measurement results; Right: simulation results

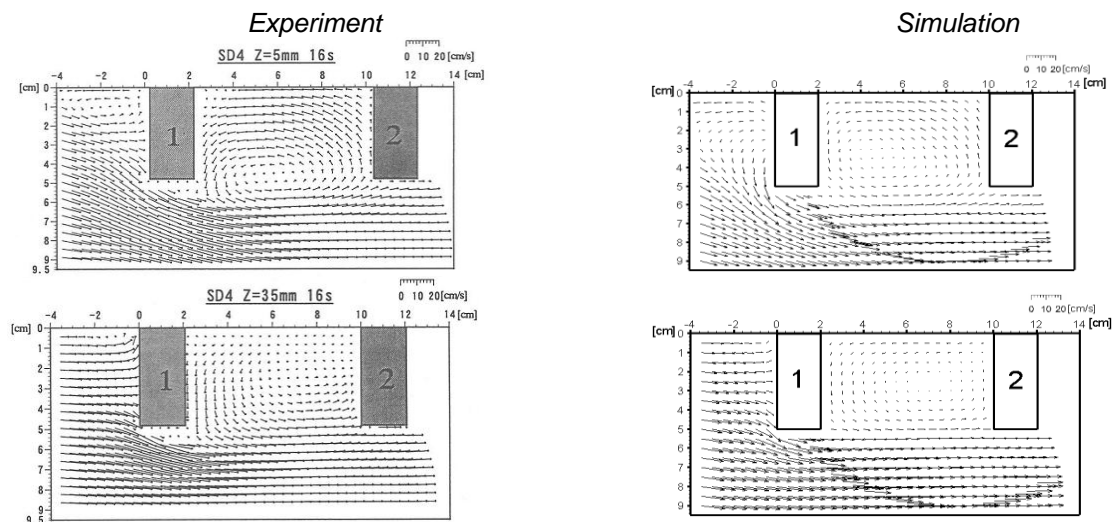


Figure 6. Velocity vector fields on Z-section. Left: measurement results; Right: simulation results

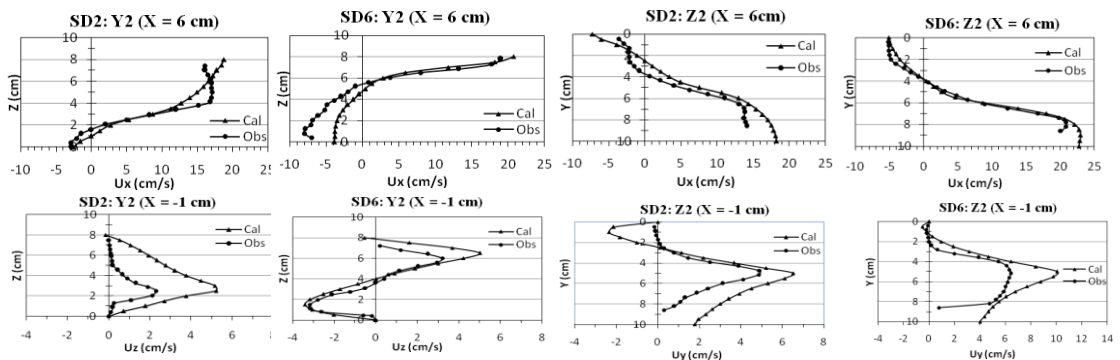


Figure 7. Vertical and transversal distribution of velocity components at different planes

Conclusion

A 3D numerical model has been described and applied for simulating the flow structure around submerged spur-dykes. The model uses a moving generalized curvilinear grid allowing it to conform to a range of curved channel and meandering river terrains. The model simulations with different configurations of submerged spur-dykes compared favourably with experimental laboratory data. It was found that the vortex formed by overtopping phenomena were reproduced well and this supports the further development of the model with the addition of sediment transport modules for more extensive application and investigation of practical river training structures.

Acknowledgements

This study was partly financed by Vietnam National University, Hanoi within the framework of research project *QGTĐ.12.07* and by DANIDA within the framework of research project *11-P04-VIE*. The first author should like to acknowledge Dr Kate Cregan and Dr Terence Chan, Monash University for their elaboration in revising this manuscript.

References

- [1] Chanson, H. (1999). *The Hydraulics of Open Channel Flow: An Introduction*. John Wiley and Sons Inc., New York
- [2] Garde, P.J. et. al., (1961). "Study of Scour around Spur-Dikes". *J. Hydraul. Div., Proceedings of ASCE*, Vol. 87(6), pp. 23-37.
- [3] Hirt, C. W., Nichols, B. D. & Romero, N. C. (1975). "SOLA - a Numerical solution algorithm for transient fluid flows". *Los Alamos Scientific Report, LA-5852*.
- [4] Kimura, I. & Hosoda, T. (2000). "Numerical simulation of flows around a surface-mounted cube by means of a non-linear k- ϵ model". *Proc. Of 9th International Symposium on Flow visualization*, Paper No.388, (CDROM).
- [5] Kimura, I., Hosoda, T., Onda, S. & Tominaga, A. (2004). "Computations of 3D turbulent flow structures around submerged spur dikes under various hydraulic conditions". Greco, M., Carravetta, A. & Della Morte, R. (eds), Napoli: Balkema, *River Flow 2004* (1), pp. 543-553.
- [6] Kuhnle, R. A., Alonso, C. V., and Shields, F. D., Jr. (1999). "Geometry of scour holes associated with 90° spur dikes". *J. Hydraul. Eng.*, Vol. 125(9), pp. 972–978.
- [7] Kwan, T. F., and Melville, B. W. (1994). "Local scour and flow measurements at bridge abutments". *J. Hydraul. Res.*, Vol. 32(5), pp. 661–673.
- [8] Leonard, B.P. (1979). "A stable and Accurate Convective Modelling Procedure Based on Quadratic Upstream Interpolation". *Comput. Meths. Appl. Mech. Eng.* Vol.19, pp. 59-98.
- [9] Lim, S. Y. (1997). "Equilibrium clear-water scour around an abutment". *J. Hydraul. Eng.*, Vol. 123(3), pp. 237–243.
- [10] Martin, J. L. and McCutcheon, S. C. (1999). *Hydrodynamics and transport for water quality modelling*. Lewis Publications, Boca Raton, Florida.
- [11] Melville, B. W. (1992). "Local scour at bridge abutments". *J. Hydraul. Eng.*, Vol. 118(4), pp. 615–631.
- [12] Nagata et al. (2005). "Three-dimensional numerical model for flow and bed deformation around river hydraulic structures". *Journal of Hydraulic Engineering*, Vol. 131, No. 12, pp. 1074–1087.
- [13] Rahman, M. M., Nagata, N., Muramoto, Y., and Murata, H. (1998). "Effect of side slope on flow and scouring around spur-dike-like structures". *Proc., 7th Int. Symp. on River Sedimentation*, Hong Kong, China, pp. 165–171.
- [14] Takizawa, A., Koshizuka, S. & Kondo, S. (1992). "Generalization of physical component boundary fitted co-ordinate (PCBFC) method for the analysis of free-surface flow". *Int. J. Num. Methods in Fluids*, Vol.(15): 1213-1237.
- [15] Tominaga A., Nakano A., Ijima K. and Nagasaka G. (2000). "Effects of relative dike height on flow structures in submerged spur-dike zones". *J. Applied Mechanics – JSCE*, Vol. 3, pp. 805-812.

Author Information

Assoc. Prof. Dr. Tran Ngoc Anh. Center for Environmental Fluid Dynamics (CEFD), VNU-Hanoi University of Science, 334 Nguyen Trai, ThanhXuan, Hanoi, Vietnam.

Assistant. Prof. Dr. Shinichiro Onda. Dept. of Urban Management, Kyoto University, Kyoto 615-8540, Japan.

BS. Nguyen Duc Hanh. Dept. of Hydrology, VNU-Hanoi University of Science, 334 Nguyen Trai, ThanhXuan, Hanoi, Vietnam.

Assoc. Prof. Dr. Nguyen Thanh Son. Dept. of Hydrology, VNU-Hanoi University of Science, 334 Nguyen Trai, ThanhXuan, Hanoi, Vietnam.